

Novel phages of *Pseudomonas syringae* unveil numerous potential auxiliary metabolic genes

Chloé Feltin^{1,*}, Julian R. Garneau², Cindy E. Morris¹, Annette Bérard³ and Clara Torres-Barceló^{1,*}

Abstract

Relatively few phages that infect plant pathogens have been isolated and investigated. The *Pseudomonas syringae* species complex is present in various environments, including plants. It can cause major crop diseases, such as bacterial canker on apricot trees. This study presents a collection of 25 unique phage genomes that infect *P. syringae*. These phages were isolated from apricot orchards with bacterial canker symptoms after enrichment with 21 strains of *P. syringae*. This collection comprises mostly virulent phages, with only three being temperate. They belong to 14 genera, 11 of which are newly discovered, and 18 new species, revealing great genetic diversity within this collection. Novel DNA packaging systems have been identified bioinformatically in one of the new phage species, but experimental confirmation is required to define the precise mechanism. Additionally, many phage genomes contain numerous potential auxiliary metabolic genes with diversified putative functions. At least three phages encode genes involved in bacterial tellurite resistance, a toxic metalloid. This suggests that viruses could play a role in bacterial stress tolerance. This research emphasizes the significance of continuing the search for new phages in the agricultural ecosystem to unravel novel ecological diversity and new gene functions. This work contributes to the foundation for future fundamental and applied research on phages infecting phytopathogenic bacteria.

INTRODUCTION

As the most abundant biological entities on the planet, the viruses of bacteria or bacteriophages (phages), play a major role in diverse ecosystems. Knowledge of these roles has provided better insight into the dynamics of diverse bacterial communities including those that govern the major biogeochemical cycles in the marine environment [1, 2], in soil [3], and in the human gut [4]. According to several studies, it has been established that phages can exert a significant influence, both quantitatively and in terms of diversification, on the host bacterial population [5, 6]. When phages are studied with respect to agriculture, they are often considered as biocontrol agents against plant pathogenic bacteria (for instance, *Xanthomonas oryzae* pv. *oryzae*: [7]; *Ralstonia solanacearum*: [8]; *Pseudomonas syringae* pv. *actinidiae*: [9]; *Pectobacterium* spp. [10]). The use of phages against bacterial diseases in agriculture was proposed very early on after their discovery [11–14]. Today's world challenges are driving the need for more sustainable agricultural solutions, such as phage-based products, which are an example of biocontrol strategy. To develop these environmentally friendly alternative solutions and better understand their interactions within microbial communities, it is necessary to identify and characterize phages.

Among the plant pathogenic bacteria that cause significant damage in agriculture, *P. syringae* is a species complex, classified into at least 13 phylogroups (PG) and 23 clades based on multilocus sequencing typing (MLST) [15]. *P. syringae* is ubiquitous and associated with ecosystems linked to the water cycle, such as lakes, rivers, clouds, snow, biofilms, soil litter, wild and cultivated plants [16]. In the latter case, this bacterium can cause losses of up to 60% in arboriculture and horticulture [17]. This pathogen can colonize leaves and other aerial plant parts as an epiphyte from which it can penetrate natural openings and wounds to attain the intercellular spaces as an endophyte. In some cases, inoculum from the endophytic phase can be devastating for the

Received 21 February 2024; Accepted 07 May 2024; Published 04 June 2024

Author affiliations: ¹INRAE, Pathologie Végétale, F-84140, Montfavet, France; ²Department of Fundamental Microbiology, University of Lausanne, CH-1015 Lausanne, Switzerland; ³Avignon Université, INRAE, EMMAH, 84914 Avignon, France.

***Correspondence:** Clara Torres-Barceló, clara.torresbarcelo@inrae.fr; Chloé Feltin, chloe.feltin@inrae.fr

Keywords: apricot orchards; auxiliary metabolic genes (AMGs); bacterial canker; Bacteriophages; *Pseudomonas syringae*.

Abbreviations: AMGs, Auxiliary Metabolic Genes; MLST, Multilocus Sequencing Typing; PG, phylogroups.

Assembled and annotated genomes of the 25 *Pseudomonas syringae* phages were uploaded to GenBank under accession numbers PP179310 to PP179334. All data generated or analysed during this study are included in this published article (and in the two "Supplementary Material" files). Five supplementary figures and four supplementary tables are available with the online version of this article.

001990 © 2024 The Authors



This is an open-access article distributed under the terms of the Creative Commons Attribution License. This article was made open access via a Publish and Read agreement between the Microbiology Society and the corresponding author's institution.

plant with sudden wilting, the presence of cankers on stems and main trunks, and the production of exudates [18]. On apricots, *P. syringae* can cause bacterial cankers, which lead to a complex and episodic disease with considerable economic impacts in several regions of the world, particularly in Iran [19], Turkey [20], Bulgaria [21] and Italy [22]. Controlling bacterial canker on apricots is difficult due to the complex nature of the disease and the responsible pathogen. The *P. syringae* strains responsible for the disease represent a high degree of genetic variability [23, 24]. On apricot tissues affected by bacterial canker, the pathogenic strains are mainly identified as PG01, PG02, and less frequently as PG03 and PG07 [23]. The pathogenicity of a strain on apricot trees cannot be predicted either by its phylogeny or by phenotypic characteristics, and phages may be playing an important, yet unknown, role.

Phages infecting human pathogenic bacteria have been studied more extensively than those infecting phytopathogenic bacteria. This can be measured by the number of phage genomes sequenced: 2017 accessions for *Escherichia coli* phages and 873 for *P. aeruginosa* phages, whereas there are only 110 *P. syringae* phage genomes (INPHARED; March 2024). The diversity of the *P. syringae* species complex is comparable to the bacterial complexes of these two other families, indicating that further diversity is yet to be discovered for *P. syringae* phages. The need to expand phage genome databases therefore remains important, as does the need to build up collections of purified phages relevant to agriculture contexts.

This imbalance is changing, as illustrated by the growing literature on phages of plant-associated bacteria. Recent studies on *P. syringae* phages have investigated their potential as biocontrol agents. For instance, the Medea1 phage represented a new genus and its biocontrol capacity was tested *in vitro* and *in planta* [25]. It was isolated from a strain of *P. syringae* pv. *tomato* from tomato seedling soil and characterized genetically and phenotypically. This new phage also showed strong antibiofilm activity. Similarly, the phage ΦPsa374 was isolated from soil and compost by enrichment with *P. syringae* pv. *actinidae* strains [9]. Their study described the ΦPsa374 genome to understand its properties and infection strategies, with the aim of using it as a durable antimicrobial agent. Warring *et al.* showed that this phage uses LPS as a receptor *in vitro* and *in planta*, and that mutations in the synthesis of these LPS are involved in resistance to phage infection [26]. Numerous mutations in the phage genome were also noted in the tail fibre and a structural protein, suggesting evolution and adaptation of the phage to the bacterial strains. ΦPsa374 genome sequencing included genes associated with tellurium resistance, a rare trait that has been reported to possess antimicrobial properties. These types of genes are auxiliary metabolic genes (AMGs) integrated into the phage genome and are likely to promote the fitness of the infected bacteria and thus indirectly enhance phage replication efficiency. Although these genes have been described in other ecological contexts (marine [27] or soil [28]), to our knowledge, no study has described AMGs in phages of plant-associated bacteria. These recent findings highlight the potential for finding phages particularly suited for biocontrol, as well as the prospect of discovering novel AMGs.

In this work, we sought to collect phages from an agricultural context where *P. syringae* is an important pathogen, viz. as the causal agent of bacterial canker of apricots. The soil of symptomatic apricot orchards was sampled and enriched with several *P. syringae* strains with the objective of detecting a wide diversity of phages. The genetic description of this phage collection was accompanied by functional genome annotation and inter-genus comparison to identify interesting characteristics of newly discovered phage genera. This new collection highlights the important genetic diversity found in *P. syringae* phages.

METHODS

Soil sampling in apricot orchards

All samples were taken in November 2021 at the INRAE experimental research unit in Gotheron (Saint-Marcel-lès-Valence, Drôme, France) in three apricot orchards. Table S1, available in the online version of this article, describes the characteristics of these orchards. Ten soil samples were taken from each orchard. Soil was sampled from the base of the tree showing symptoms of bacterial canker (within a perimeter of approximately 30 cm at a depth of approximately 10 cm (one 50 ml Falcon tube per sample from the first layer of soil or the A horizon). The soils had a cation exchange capacity of 12.2 meq/100 g, a neutral pH (pH water 7.0) and an organic matter level of 1.9%.

Selection of bacterial strains and culture conditions

Twenty-one strains of *P. syringae* from the Plant Pathology Research Unit (INRAE, Montfavet, France) collection were used for phage isolation (Table 1). It should be noted that those bacterial strains were not isolated during the course of that study. These strains reflect the genetic diversity of *P. syringae* on apricot (Table 1) [23]. It also included *P. syringae* strains isolated from other host plants and from aquatic environments genetically close to strains isolated on apricot on the basis of the sequence of the housekeeping gene citrate synthase (*cts*) (Table 1). Phylogenetic analyses were conducted using MEGA version 11 [29] by building a neighbour-joining tree with 1000 bootstraps using the *p*-distance method and rooted with strains outside of the species complex. All the strains belong to five different phylogroups (PG01, PG02, PG03, PG07, PG10) with at least three strains per phylogroup except for PG10 (Table 1). *P. syringae* strains were stored at -80°C in phosphate buffer with glycerol (20% vol/vol). They were cultured on King's B (KB) agar medium [30] for 48 h at 25°C before each experiment.

Table 1. The 21 strains of *P. syringae* used for the phage isolation enrichment step. The isolation characteristics of *P. syringae* strains are presented as well as phylogenetic and phenotypic traits

Environment of origin	Names	CFBP collection	Phylogroup	Pathogenicity ^a	Country of isolation	Date of isolation	Plant and environment of isolation	No. of phage isolates
Haplotypes isolated from apricot trees	DG1a.21		PG01a	+	France	13/04/2015	<i>Prunus armeniaca</i>	5
	P1.01.01B03		PG01a	-	France	01/03/2014	<i>Prunus armeniaca</i>	14
	19B		PG01a	+	France	16/03/2011	<i>Prunus armeniaca</i>	4
	P3.01.09C09		PG01a	-	France	01/03/2014	<i>Prunus armeniaca</i>	15
	41A		PG02b	+	France	14/04/2011	<i>Prunus armeniaca</i>	0
	P4.01.01C03		PG02b	-	France	01/05/2014	<i>Prunus armeniaca</i>	9
	DG12.6		PG02d	+	France	13/04/2015	<i>Prunus armeniaca</i>	17
	7C		PG02d	+	France	16/03/2011	<i>Prunus armeniaca</i>	22
	DG8.15		PG07	+	France	13/04/2015	<i>Prunus armeniaca</i>	7
	3A		PG07	-	France	16/03/2011	<i>Prunus armeniaca</i>	4
	93D		PG07	+	France	14/04/2011	<i>Prunus armeniaca</i>	10
93A		PG03	+	France	14/04/2011	<i>Prunus armeniaca</i>	9	
Haplotypes isolated from other plants	CC1630	CFBP 8561	PG01a	NT	USA	27/10/2007	<i>Onobrychis viciifolia</i>	0
	DC3000	CFBP 7438	PG01a	NT	United Kingdom	01/01/1960	<i>Solanum lycopersicum</i>	1
	CC0440	CFBP 8573	PG02b	NT	France	13/06/2002	<i>Cucumis melo</i>	4
	CC0094	CFBP 5467	PG02d	NT	France	22/06/1997	<i>Clematis patens</i>	18
	CC0663		PG07	NT	France	20/04/2004	<i>Primula officinalis</i>	23
	JD03	CFBP 8535	PG03	NT	USA	01/01/1977	<i>Glycine max</i>	9
	Pph1448A		PG03	NT	Ethiopia	01/01/1985	<i>Phaseolus vulgaris</i>	13
Haplotypes isolated from water environments	USA0011	CFBP 8553	PG02d	NT	USA	12/08/2007	River	16
	CC1557	CFBP 8533	PG10b	NT	France	20/06/2006	Rain	23

If present in the CFBP collection, the strain's reference number in that collection is provided. The CIRM-CFBP is the French collection for plant-associated bacteria (<https://cirm-cfbp.fr/>; Feb 2024). The pathogenicity of the strains on apricot trees is detailed as described by Parisi et al. [23]; NT = not tested; + = pathogenic; - = not pathogenic.

Phage isolation

The 30 soil samples were stored at 4°C in 50 ml Falcon tubes for 3 weeks. Isolation was carried out according to standard protocols [31]. Briefly, the homogenization phase consisted of mixing approximately 50 g of soil with 110 ml of liquid KB medium with slow agitation for 1 h at 25°C. The supernatant was centrifuged (3215 g for 5 min) and then filtered (Merck Millex Syringe Filter, PES, 0.22 µm). In the enrichment phase, this filtrate was mixed with each of the 21 *P. syringae* strains (Table 1) in exponential phase (OD=0.2 corresponding to approximately 10⁸ c.f.u. ml⁻¹). This mixture was incubated at 25°C for 48 h with slow agitation. Only the phages were kept by adding 10% chloroform, then vortexing and centrifuging (16873 g for 5 min) to retain the supernatant. To observe the presence of phage in these enrichments, screening was carried out with the 'spot test' technique using the double-layer agar method [32]. From the 221 positive screening tests showing halos of bacterial lysis, 89 were selected for phage purification, representing a variety of strains of *P. syringae* and soil samples. To purify phages, p.f.u. (bacterial lysis plaque-forming units) were isolated three consecutive times using the double-layer agar method. A total of 50 phages (56%) were isolated and purified in 100 µl of SM buffer (100 mM NaCl, 8 mM, Mg SO₄ 7H₂O, 50 mM Tris-HCl, pH 7.4). Finally, phages were amplified at a titre ranging from 10⁴ p.f.u. ml⁻¹ to 10¹¹ p.f.u. ml⁻¹. The selection of reference species phages was based on those with a high p.f.u. ml⁻¹ titre that remain stable over time. The phage collection was stored at 4°C in SM buffer and at -80°C in glycerol (50% vol/vol).

In addition, attempts were made to isolate phages from the soil of asymptomatic trees, but the lysis plaques were too turbid to purify the phages. Therefore, no phages were purified from the soil of asymptomatic trees.

Phage morphology observed by TEM

Electron micrographs of *P. syringae* phages were generated as previously described [33]. Briefly, the sample was placed on a 400-mesh copper grids (Delta microscopies, Mauressac, French), negative stained with 1% (W/V) ammonium molybdate, and analysed using a HT7800 Hitachi transmission electron microscope (Hitachi, Tokyo, Japan) at an acceleration voltage of 80 kV. Electron micrographs were taken with an AMT XR401, sCMOS-camera (AMT imaging, Woburn, MA-US).

DNA extraction

DNA was extracted from the 50 phages in the collection using either the Phage DNA Isolation kit (Norgen Biotek CORP) or a phenol-chloroform protocol from pure amplified phages. The quantity and quality of the extracted DNA was checked with a nanodrop spectrophotometer (ND-1000 Spectrophotometer), Qbit (3.0 Fluometer) and the DNA was visualized on a gel (1% agarose). The DNA of the 50 phages was then sent to the Biomix sequencing platform at the Pasteur Institute (Paris, France). The libraries were prepared using Illumina TruSeq PCR-Free and sequencing was carried out using ISeq100 PE150 (2×150 pb read length, target 100 X / sample). Of the 50 genomes, 38 were successfully sequenced and assembled.

Phage genome assembly and annotation

Sequence analysis was performed on Galaxy CPT [34] and genome assembly was performed *de novo* with the Trimmomatic [35], SPAdes [36], PhageTerm [37] tools. Phage morphology was determined with VIRFAM [38]. The phage life cycle was identified with PhageAI (Table S3) [39]. The comparison of genomes by inter-genomic distances allowed us to analyse the taxonomy of our collection of 38 phages sequenced relative to close reference phages currently known (VIRIDIC) [40]. The functional annotation of phages was updated using PROKKA [41] with a priority annotation using a modified PHASTER protein database (version Dec 22; [42]). To increase the number of identifiable ORF, hypothetical proteins were removed, and the E-value threshold for function assignment was set to 0.01. The predicted function of all genes was manually categorized (Table S4), which also led to the identification of potential AMGs. These potential AMGs were verified by comparing the protein sizes present in the phage and host genomes and by homologous comparison with a strict identity threshold of 70% and coverage of 90%. The INPHARED database was used to count the number of phages infecting *P. syringae* [43].

RESULTS AND DISCUSSION

Phages were found in all apricot soils when screened against 21 strains of *P. syringae*

To increase the likelihood of isolating a diverse range of phages, 21 strains of *P. syringae*, representing a wide range of diversity, were each added to all sampled soil (Table 1). For the total of 630 enrichments that were screened (30 soil samples × 21 host strains), 221 (35%) yielded a phage isolate and 100% of the soils yielded *P. syringae* phage isolates (i.e. at least one phage isolate in each soil sample could attack one of the *P. syringae* strains used for enrichment). An average of seven phage isolates were counted per soil, regardless of the orchard sampled. Moreover, the number of phages isolated was similar between the three orchards, with 76 in the hybrid orchard (34%), 78 in the CapRED orchard (35%) and 67 in the core collection orchard (30%), revealing that there was no effect of orchard on the number of phage isolates (Fig. S1). This result is not surprising given that the orchards sampled are very close geographically and therefore share climatic and soil characteristics, differing only in the genotype of the apricot trees. Our results prove that the isolation of *P. syringae* phages from soil is efficient. Indeed, it has been shown that *P. syringae* phages are easily isolated from soils and from water samples [44, 45]. A similar study sampled 70 isolates of *P. syringae* phages from 60 cherry trees (soil, leaves and bark) in six different geographical locations [46]. Their results were similar to ours since all soil samples yielded phages of *P. syringae*. However, in contrast with our results, the distribution of the number of phages isolated by geographical site was not uniform (45, 26, 16, 7, 4 and 2%). This result probably depends on the sampling design and accounts for the diversity of climate, soil, type of farm, number of enrichment strains, and geographical distance between sites.

The relatively wide diversity of *P. syringae* strains used to enrich the phages in the 30 soils sampled from three apricot orchards made it possible to isolate a large diversity of phages (Table 1). Of the 21 strains of *P. syringae* used, 19 were host to at least one phage (Table 1). On average, each bacterial strain was able to isolate 11 phages from the three orchards. Strain JD03 (PG03) was the most efficient at isolating phages, having isolated 23 phages from the three orchards. Strain 7C (PG02b) was also highly efficient, allowing the isolation of 22 phages (Table 1). In contrast, strains CC1630 (PG01a) and 41A (PG02b) did not yield any phage (Table 1). Parisi *et al.* tested 7C and 41A for their ability to cause disease on apricots, as well as beans, melons, tomatoes, and cherries [23]. As they have the same host range on the plants tested, pathogenicity does not appear to be linked with their ability to isolate phages. There is no evidence to suggest that a strain of *P. syringae* will be effective in isolating phages according to the habitat (e.g. plants vs water) from which they were isolated (Table 1). This reflects the fact that the *P. syringae* complex as a whole shows no biogeographical specificity and populations have been mixed among the various substrates in which it can be

found [47]. In this work, we find no differences in phage isolation between pathogenic and non-pathogenic strains on apricots. This result was expected since the diversity of *P. syringae* on apricots mainly comprises non-pathogenic strains [23].

Bacteria from all phylogroups were able to isolate phages, with PG02 isolating the highest percentage (38%) followed by PG07 (19%), PG03 (19%), PG01 (18%), and PG10 (7%) (Table 1, Fig. S1). In addition, there was no bacterial phylogenetic pattern that influenced the number of phages isolated. These results justify our approach and our choice of *P. syringae* strains, as they almost all contributed to the diversity of phages collected. The genetic diversity of populations of *P. syringae* on apricot trees is large and represents four phylogroups of the species complex [23]. Phages were isolated from all of them, indicating their ubiquitous presence in the soil of apricot trees. Even if *P. syringae* strains tend to have low residence time in soil [48], rainwater run-off could potentially create a temporary reservoir for them and hence, for their associated phages.

***P. syringae* phages from apricot soils represent 11 new genera and 18 new species**

A taxonomic analysis of the pure phages indicated a significant amount of novelty and diversity among the phages collected. Calculation of the genetic identity between the 38 purified phages indicated that 66% were unique clones representing 25 unique *P. syringae* phages. The phages belong to 18 new species and 14 genera, 11 of which are new according to ICTV criteria [49] (Fig. S2), testifying to the great taxonomic diversity of this new collection (Table 2). All of the phages in the collection belong to the class of *Caudoviricetes* (Phylum: *Uroviricota*, Kingdom: *Heunggongvirae*, Realm: *Duplodnaviria*) and therefore have the three best-known morphologies: podovirus (52%), myovirus (32%) and siphovirus (16%) (Fig. S3). The 11 new genera have been named after constellations and the 18 new species have been named after the stars that make up the constellations (Table 2).

To estimate the sampling effort for this study, we compared the number of enrichment strains and the sites sampled to those of a similar study. In their study, Rabiey *et al.* revealed that the 13 purified phages belonged to five different genera [46]. They were obtained from six cherry orchards located in six different geographical sites using three enrichment strains. Rabiey's approach isolated five phage genera for three enrichment bacterial strains ($5/3=1.67$), while our approach yielded 14 genera for 21 enrichment strains ($14/21=0.67$). However, the majority of our diversity was obtained at a single site whereas six different sites with ten varieties sampled were required to capture the diversity obtained by Rabiey *et al.* Considering only the intrinsic diversity of the two collections, ours contains 14 genera for 25 unique phages ($25/14=1.79$), compared to five genera for 13 unique phages ($13/5=2.60$). As a result, our collection has greater intrinsic diversity due to the lower number of phages per genus and the higher number of genera. For our study, we hypothesized that a high diversity of *P. syringae* phages would require a large number of different enrichment strains compared to other studies that typically used only one or two bacterial strains [25, 26, 50]. Yet, to increase the diversity of *P. syringae* phages with an efficient sampling effort, it seems that using at least three enrichment strains (instead of 21) from a single geographical site would enable the collection of many distinct genera of *P. syringae* phages. However, additional phage sampling and enrichment projects should be conducted at contrasted sites to confirm this hypothesis.

The taxonomic diversity of our collection of 25 *P. syringae* phages was analysed at the genus level. There was no inter-genomic similarity between the 14 genera, except for the *Lepusvirus* genus phage, which shared around 58% inter-genetic similarity with the phage belonging to the *Ghunavirus* genus, and the *Aurigavirus* genus phage, which shared 69% with the *Cruxvirus* genus phage (see Fig. S2). This differentiation between almost all genera was further highlighted by comparing our collection with existing phages in databases, as shown in Fig. 1. The phages in the collection were widely distributed in the proteomic tree and the closest phages related to ours originated from various hosts, such as *Pseudomonas*, *Escherichia*, *Acinetobacter*, *Bordetella*, *Aeromonas*, *Ralstonia*, and *Erwinia* (Fig. 1). Out of the 11 new genera, six are represented by only one phage clone. Only three of these six genera are composed of temperate phages, indicating a misrepresentation of these *P. syringae* phages. The genera *Dracovirus* and *Orionvirus* are unique in that the isolation strain is common to all four clones of phages within those two genera (CC0094 for *Dracovirus* and 7C for *Orionvirus*, both from phylogroup 02d).

Fig. 2 displays the contribution of each enrichment strain to the phage collection for the 38 non-unique phages thereby illustrating how different *P. syringae* strains lead to isolation of identical phage clones. The *Uliginivirus tursei* Ulitu01 phage demonstrates this phenomenon with P4.01.01C03 (PG02b) as the isolation strain and a 100% identical phage clone isolated from the CC0440 (PG02b) enrichment strain. Similarly, the *Nickievirus ankaa* Nican01 phage was isolated from enrichment strain CC0094 (PG02d) and a 100% identical phage was isolated from strain 3A (PG07). The *P. syringae* strains that isolated those phage clones are from completely different phylogroups and were isolated from different plant species. The multiplicity of enrichment strains enabled us to postulate that those strains will be included in the host range of the two unique phages presented below.

***P. syringae* phages exhibit a range of genomic size and potential new termini**

The size of the genomes and their relationship with existing phages in the GenBank database are the first characteristics that distinguish the different genera in our phage collection. The median genome size was 47.123 kb (*Lyravirus sulafat*), ranging from 41.446 kb (*Ghunavirus alcor*) for the smallest to 166.013 kb (*Cygnusvirus sadr*) for the largest (see Table 2). Our collection of phages had an average GC percentage of 54%, with *Pyxisvirus pyxidis* having the lowest at 46% and *Toucanavirus emiw*,

Table 2. Genetic characteristics of 25 *P. syringae* phages

Clones	Species	Genera	Genome size (pb)	% GC	Terminus	Morphology	No. of CDS	% of known functions	No. of tRNA	GenBank accession
<i>Arace01</i>	<i>Aravirus</i>	cervantes	76815	51%	DTR (short)	podovirus	84	53.57	2	PPI79312
<i>Aurca01</i>	<i>Aurigavirus</i>	capella	57369	58%	-	siphovirus	94	43.62	0	PPI79334
<i>Cruim01</i>	<i>Cruxivirus</i>	imai	55644	58%	-	siphovirus	87	42.53	0	PPI79333
<i>Cygsa01</i>	<i>Cygnusvirus</i>	sadr	166013	57%	-	myovirus	256	27.73	3	PPI79332
<i>Draal01</i>	<i>Dracovirus</i>	altais	43777	56%	Headful (pac)	podovirus	58	51.72	0	PPI79322
<i>Draal02</i>	<i>Dracovirus</i>	altais	43779	56%	-	podovirus	57	43.86	1	PPI79321
<i>Draal03</i>	<i>Dracovirus</i>	altais	43779	56%	-	podovirus	57	43.86	1	PPI79319
<i>Dracl01</i>	<i>Dracovirus</i>	eltanin	42756	56%	Headful (pac)	podovirus	54	53.70	0	PPI79320
<i>Ghua01</i>	<i>Ghnavivirus</i>	alcor	41446	56%	Headful (pac)	podovirus	49	73.47	0	PPI79313
<i>Ghuch01</i>	<i>Ghnavivirus</i>	chalawan	41728	56%	DTR (short)	podovirus	50	72.00	0	PPI79330
<i>Lepni01</i>	<i>Lepusvirus</i>	nihal	41894	57%	DTR (short)	podovirus	47	74.47	0	PPI79331
<i>Lyrsa01</i>	<i>Lyravirus</i>	sulafat	47123	52%	New	podovirus	66	37.88	1	PPI79323
<i>Lyrsa02</i>	<i>Lyravirus</i>	sulafat	47123	52%	New	podovirus	66	37.88	1	PPI79324
<i>Lyrsa03</i>	<i>Lyravirus</i>	sulafat	47206	52%	New	podovirus	66	37.88	1	PPI79314
<i>Nican01</i>	<i>Nickievirus</i>	ankaa	112436	57%	DTR (long)	siphovirus	165	28.48	5	PPI79318
<i>Orimi01</i>	<i>Orionvirus</i>	mintaka	46001	55%	-	myovirus	76	43.42	0	PPI79326
<i>Orisa01</i>	<i>Orionvirus</i>	saiph	45336	54%	-	myovirus	75	46.67	0	PPI79329
<i>Orisa02</i>	<i>Orionvirus</i>	saiph	45363	54%	-	myovirus	74	47.30	0	PPI79328
<i>Orisa03</i>	<i>Orionvirus</i>	saiph	44995	54%	-	myovirus	68	47.06	0	PPI79327
<i>Pawpe01</i>	<i>Pavovirus</i>	peacock	44080	53%	Headful (pac)	siphovirus	54	61.11	0	PPI79316
<i>Pyxpy01</i>	<i>Pyxisvirus</i>	pyxidis	101236	46%	DTR (short)	myovirus	204	32.35	19	PPI79310
<i>Pyxpy02</i>	<i>Pyxisvirus</i>	pyxidis	99504	46%	DTR (short)	myovirus	191	34.55	6	PPI79311
<i>Touem01</i>	<i>Toucanavirus</i>	emiw	91577	58%	Headful (pac)	myovirus	128	32.81	0	PPI79325
<i>Ulna01</i>	<i>Uliginivirus</i>	naos	47685	56%	DTR (short)	podovirus	48	68.75	0	PPI79315
<i>Ulitu01</i>	<i>Uliginivirus</i>	turais	47775	56%	DTR (short)	podovirus	47	68.09	0	PPI79317

The phages in bold have been predicted as temperate whereas the others are predicted as virulent.

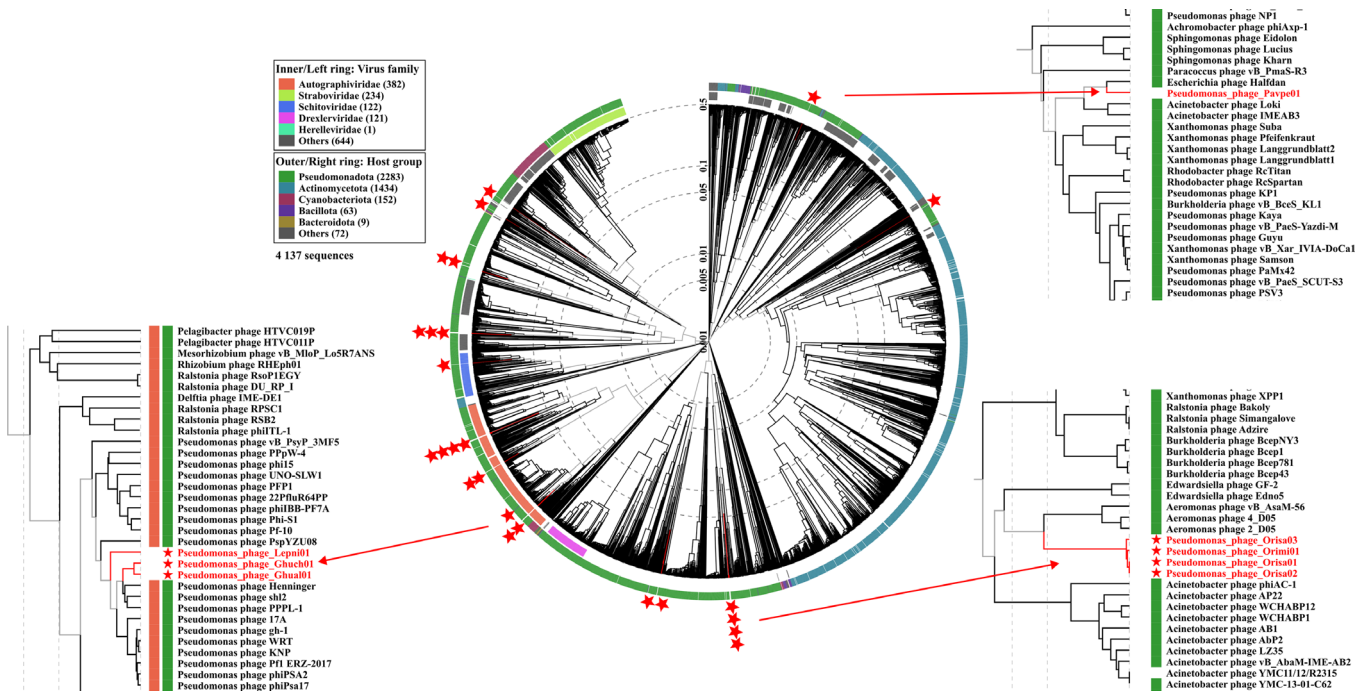


Fig. 1. Proteomic tree of the phylogenetic context of 25 newly discovered *P. syringae* phage genomes (indicated by red stars), generated with VipTree and modified with Inkscape version 1.3.2. The inner ring represents the known virus families of the related phage genomes, while the outer ring shows the host group of these phages. Enlarging three groups highlighted some phages close to those in the collection. Phages are indicated with their respective GenBank accession identifiers.

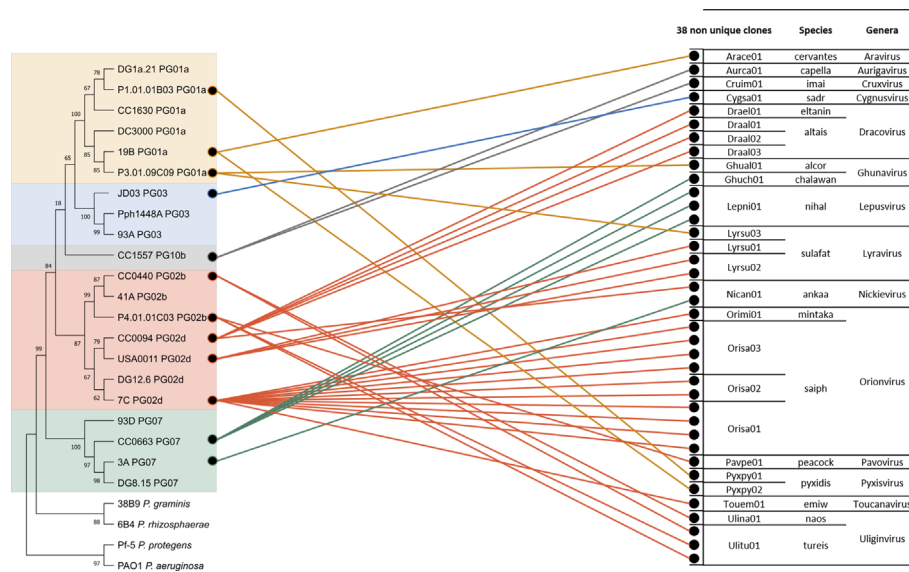


Fig. 2. Network between the enrichment strains of *P. syringae* on the left and the 38 non-unique *P. syringae* phages on the right. The *P. syringae* strains are represented in a neighbour-joining tree from the housekeeping cts (citrate synthase) gene and rooted with strains outside of the species complex. The four phylogroups in this tree are delimited by different coloured backgrounds (yellow: PG01a, blue: PG03, pink: PG02b and d, grey: PG10b, green: PG07). The phage collection includes 38 non-unique phages, identified by a dot and named after their reference phage clone. Phages are classified according to their species and genus.

Cruxvirus imai and *Aurigavirus capella* having the highest (58%). Furthermore, the GC content of the three temperate phages is the most similar to that of their host *P. syringae*, averaging at 59% across 58 complete genomes (GenBank; Jan 2024). It is worth noting that temperate phages often have a GC content that is more similar to that of their host than virulent phages [51].

A comparison of the phages in the collection with the 15 most closely related phages in the GenBank database is presented in Table S2. The phage genera *Uliginivirus*, *Nickievirus*, and *Ghunavirus* have a high degree of similarity and extensive coverage with phages in the database, indicating that those genera have been previously described (Fig. S4). Phage *Cruxvirus imai* Cruim01 shows a high level of identity with the bacterium *P. syringae*, due to the presence of homologous prophages sequence in the bacterial genome. It was predicted that *Cruxvirus imai* Cruim01 has a lysogenic lifestyle (Table S3), which is further supported by the homology of this phage with the host genome. Indeed, a recent study showed that in around 99.3% of the genomes of roughly 1500 *P. viridiflava* ATUE5 that were isolated from *Arabidopsis thaliana*, there were on average two prophage sequences per bacterial genome [52]. According to another study, which analysed 13713 bacterial genomes, the average number of prophages per genome is 3.24 [53]. Finally, a recent study has shown that deleterious prophages in the *P. syringae* genome, which are incomplete phage genomes, can still be utilized by the bacterium in the form of tailocins to kill sensitive strains [54].

This phage collection has an interesting genomic characteristic related to packaging systems of their DNA in their capsids (Table 2). The genomes of our collection have two types of packaging mechanisms: direct terminal repeats (DTR) present in 32% of the phages and headful without a pac site present in 20%. These mechanisms are used by double-stranded DNA phages to circularize their genomic DNA after injection in the host bacterial cell [37]. In contrast, in 36% of the phages, no termini system was identified. In these cases, the terminase gene was conventionally used as the genome origin [55]. In addition, the Lyrso02 clone appear to have an unusual 5' COS-like motif with 190 base-pair cohesive sequences (Fig. S5). It is worth noting that no known phage with cohesive sequences longer than 20 bp has been described so far. The Lyrso01 clone also showed unusual packaging features, with the potential presence of two very distinct termini in the same genome: a 190 bp 5' COS motif like Lyrso02 and a 3' COS motif (Fig. S5). Further experimental investigation is required to confirm the identification of these potential new termini in this *Lyravirus sulafat* species.

***P. syringae* phages have consistent gene architecture within each genus and they possess various auxiliary metabolic genes (AMGs)**

The phage genomes in our collection were compared based on functional annotations and their assignment to functional modules, including DNA metabolism, host lysis, lysogeny, potential auxiliary metabolic genes (AMGs), and structure, packaging, and assembly (refer to Table S4). After annotation, an average of 48.2% of the proteins have been annotated with a putative known function. In general, functional annotations for *P. syringae* phages are limited due to inadequate and poor databases, which requires further study [45].

The gene architecture and synteny of phages is conserved within the same genus, but each genus has a specific diversity of architectures (Fig. 3). Furthermore, the six genera with a single phage clone that cannot be compared were not further detailed in this section.

The four phages in the *Orionvirus* genus share at least 95% inter-genomic similarity in the *saiph* species and 94% between *mintaka* and *saiph* species. The primary distinction between these two species is the existence of an endonuclease (*Pseudomonas*_phage_Orimi01_00054) and a putative ERF family protein (*Pseudomonas*_phage_Orimi01_00055) in *Orionvirus mintaka*, which are associated with DNA metabolism and are not present in the other species. One notable characteristic of this genus in the host lysis functional module is the presence of a lysozyme that catalyses the destruction of the bacterial cell wall, followed by the o-spanin protein that disrupts the outer membrane. In the Orisa03 phage, this protein is divided into two parts: the inner membrane spanin component (*Pseudomonas*_phage_Orisa03_00034) and the outer membrane spanin component (*Pseudomonas*_phage_Orisa03_00035) [56].

The *Dracovirus* genus comprises four distinct phages across two species: *altais*, which is composed of nearly identical clones (99.9% similarity), and *eltanin*, which shares 94.8% similarity with the *altais* species. This genus of the phage has two interesting distinctive features: the presence of two proteins involved in DNA metabolism (HNH homing endonucleases) and a host lysis module composed of a lysozyme and a putative Rz-like protein involved in the final step of bacterial lysis [57]. *Toucanavirus emiw* also possesses the HNH homing endonuclease protein. One difference between the two species is that *Dracovirus eltanin* lacks a block of four consecutive genes, consisting of three hypothetical proteins followed by a putative acetyltransferase of unknown function.

The *Lyravirus sulafat* species is composed of three distinct phages (with 99% similarity) that share most of their genes, with only a few differences in hypothetical proteins. The same applies to the *Pyxisvirus pyxidis* species (99% identity), which consists of two very similar phages. A notable difference in this genus is the high number of tRNAs in phage Pyxpy01, which has 19 compared to six in Pyxpy02 (Table 2). This could explain the 1732 nucleotide difference in genome size for Pyxpy01. This genus has a higher abundance

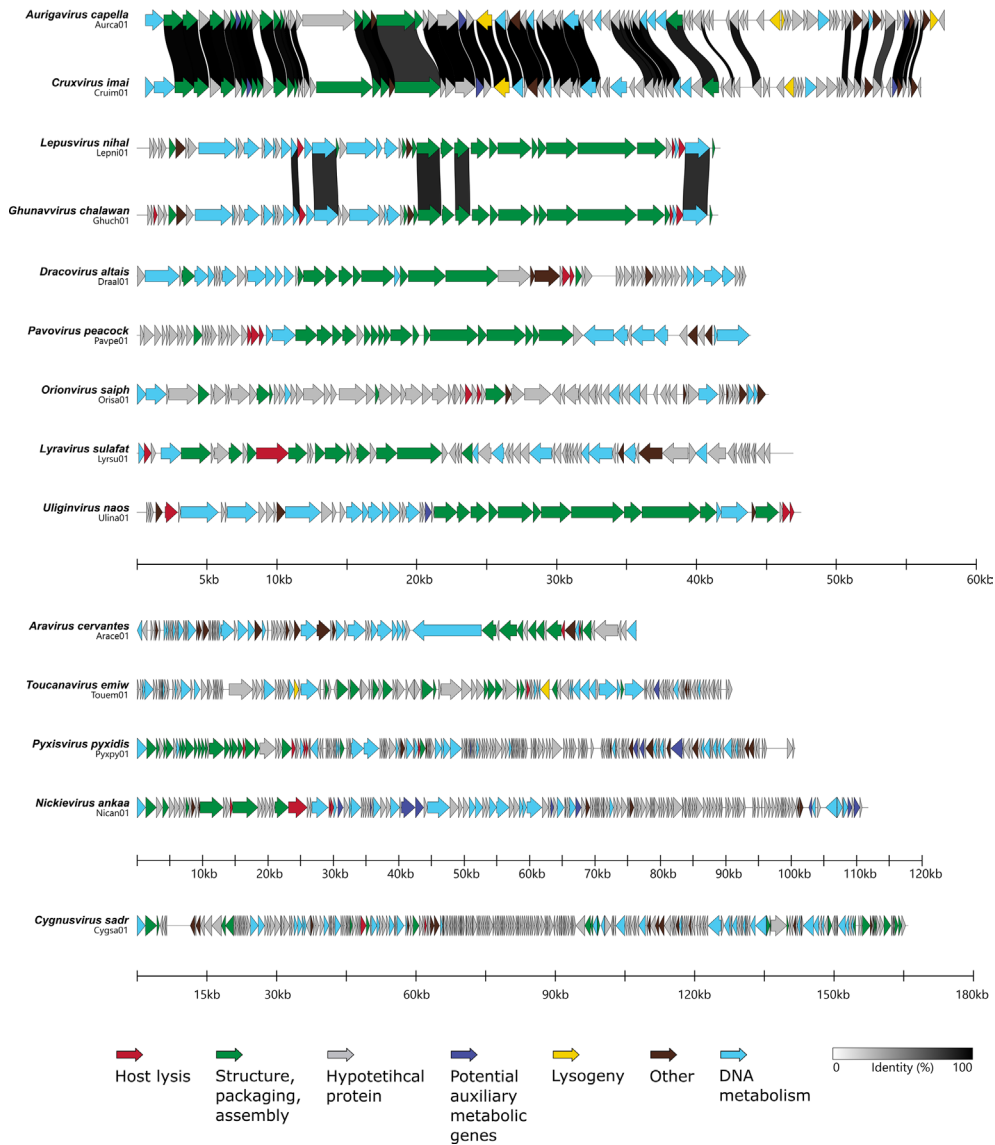


Fig. 3. Comparison of the structures of 14 genomes representing the 14 *P. syringae* genera made with Clinker and modified with Inkscape version 1.3.2. The arrows indicate the open reading frame and the direction. Functional modules are indicated and categorized by coloured arrows. Links for shared identity between proteins are presented as black to white bands and protein identity lower than 80 % is not shown.

of tRNA compared to the average of 1.6 tRNAs per genome in the collection. Phages use their own DNA and RNA polymerase, but rely on the host cell for protein synthesis. It is surprising to find tRNAs in phage genomes, but their roles have been found to improve the synthesis of viral proteins [58]. Our dataset also shows that temperate phages have fewer tRNAs than virulent phages, likely due to their GC content similar to the host [51].

Additionally, the genus *Ghunavirus* currently has ten species listed on the ICTV (as of Jan 2024), with two new species being described in this study. All species in this genus share the functional module of structure, packaging, and assembly, as well as the host lysis module (type II holin and an Rz-like lysis protein). However, there are significant nucleotide differences between species in the tail fibre protein, which could indicate a different range of phage hosts within this genus [59].

Certain phages exhibit similar gene architectures despite belonging to different genera. For instance, the genera *Aurigavirus* and *Cruxvirus* share a gene architecture (Fig. 3) and have an intergenomic similarity of 68.90%. Similarly, the genera *Ghunavirus* and *Lepusvirus* share a gene architecture and have an intergenomic similarity of 58.72%. The high genetic homology between the phage genera *Ghunavirus* and *Lepusvirus*, and the phage genera *Aurigavirus* and *Cruxvirus*, may indicate a speciation event. It is plausible that these two pairs of genera were a single genus before, and speciation driven by an active host-virus dynamic has allowed them to

diversify [60]. This argument is suggested in particular because they share the bacterial host of isolation (CC1557 from PG10b for the *Aurigavirus* and *Cruxvirus* genera; CC0663 from PG07 for the *Ghunavirus* and *Lepusvirus* genera). Research conducted by de Leeuw *et al.* demonstrated that a phage isolated from a particular strain can enhance its predation efficiency of a different bacterial strain by selecting mutations in the tail-related region [61].

The prediction of the phage lifestyle aligns with the functions of the associated genes found in their genomes (Table S3). Out of the 25 phages, 22 have a predicted lytic lifestyle, while the remaining three are predicted as the temperate phage, each containing at least one integrase. *Cruxvirus imai* Cruim01 also has a CII repressor, *Toucanavirus emiw* Touem01 has a ParA-like partition protein, and *Aurigavirus capella* Aurca01 has a CI repressor, a Cro-like protein, and a putative transposase [62]. However, the validation of their lysogenic lifestyle still needs experimental verification of integration in the host genome or maintenance as an episome in the host cell. Additionally, only 3 out of 25 phages were predicted as temperate, which is only 12%. Isolating and purifying from turbid plaques can be more challenging than from clear ones. The low infection capacity of some phages, which results in the formation of turbid plaques, is often associated with a lysogenic lifestyle. However, plaque morphology is not only linked to the lifestyle but also to the culture medium used and the physiological state of the bacterial host [63].

The present study identifies potential AMGs within phage genomes. These genes can regulate host-cell metabolism upon infection and modulate phage replication efficiency. These genes are acquired by phages via horizontal transfer from their bacterial host [64]. Thus, the detected AMGs exhibit strong homologies with other *P. syringae* phage proteins and with the host bacterium. AMGs have been extensively studied in aquatic ecosystems, the best-known example being the cyanophages, which encode numerous genes involved in biological processes like photosynthesis, stress tolerance, nucleic acid synthesis, carbon and cellular metabolism to enhance the growth of their host [27]. Our study of the 25 *P. syringae* phage genomes revealed 26 potential AMGs, but only four genes have exactly the same length as the homologue in the database, raising questions about their functionality. Nevertheless, it should be noted that the threshold used to validate potential AMGs from this phage collection is stricter than in other studies [65].

The 26 potential AMGs in our *P. syringae* phages genomes can be classified into three putative functional categories: cellular metabolism (61.5%), stress tolerance (26.9%), and nucleic acid synthesis (11.5%), as presented in Table 3. Three different AMGs (one is found twice) in particular are likely to be complete and have a high number of hits with *Pseudomonas* bacteria in two of our temperate phages: the *Aurigavirus capella* Aurca01 and *Cruxvirus imai* Cruim01 phages. The first one is a gene encoding the putative function of glutamate 5-kinase (*Pseudomonas*_phage_Aurca01_00008 and *Pseudomonas*_phage_Cruim01_00009). It is involved in osmotic protection as it catalyses and controls proline synthesis [66]. The second encodes a potential chemotaxis function (*Pseudomonas*_phage_Aurca01_00088 and *Pseudomonas*_phage_Cruim01_00082) that is involved in bacterial motility. This is the process by which bacteria move along gradients of attraction and can aid in their escape from non-motile phages that are diffusing [67].

Among all the phages, Nican01 has the highest number of potential AMGs, with nine identified in its genome, belonging to all three putative functional categories. A common gene within the *Nickievirus* genus genomes encodes a photosystem I complex protein (*Pseudomonas*_phage_Nican01_00067), with the potential to enhance host photosynthesis and material biosynthesis. This gene is present in plants, cyanobacteria, and their associated phages [68]. For instance, it was demonstrated that phage S-PM2 encodes AMGs *psbA* and *psbD*, which are homologues of bacterial photosynthetic proteins II D1 and D2 [69]. Bacteria infected with this phage are able to maintain their photosynthetic capacity thanks to the phage's AMGs until lysis [70]. The presence of this photosynthesis-associated gene in genomes of phages of *P. syringae* is unexpected and requires further investigation.

Interestingly, *Nickievirus* genus phages code for a tellurite resistance protein (*Pseudomonas*_phage_Nican01_00150) and the *Pyxisvirus* genus ones contain a gene that codes for an integral membrane protein of the *terC* family (*Pseudomonas*_phage_Pyxy01_00144 and *Pseudomonas*_phage_Pyxy02_00144 with a size of 224 aa). The *terC* gene (whole *terC* gene = 346 aa) is one of seven genes that comprise the bacterial tellurite resistance determinant in plasmid R478 (*terZABCDEF*) [71]. This plasmid is present in several bacteria of the *Enterobacteriaceae* family and in the opportunistic bacterium *Serratia marcescens*, from which the plasmid was originally isolated. The *tmp* gene (218 aa) is the bacterial tellurite resistance determinant in the *P. syringae* genome, but it is not present in the genomes of *P. syringae* phages. According to Peng *et al.*, those genes are classified as stress-tolerance due to the toxicity of tellurite, a metalloid, to bacteria among other organisms [72].

It is important to recall that the presence of incomplete genes involved in tellurite resistance in phage genomes does not necessarily indicate that phages can provide this resistance. Indeed, the function of these genes in bacterial genomes, and particularly in phage genomes, is not yet fully understood [71]. Nevertheless, one hypothesis suggests that these potential AMGs present in phage genomes may increase or maintain tellurite resistance in infected bacteria. It has been advocated that a high abundance of AMGs would be selected in soils stressed by organochlorine pesticide pollution [65], as they would increase host fitness. This could imply that the soil of apricot trees presenting symptoms of bacterial canker constitutes a stressful environment for the bacteria due to the high proportion of AMGs found in the phage genome.

In summary, 8 out of 25 phages (32%) have potential AMGs present in their genome. It should be noted that there is currently a lack of a database and pipeline to annotate and identify AMGs in a robust and reliable manner [28]. Future research could aim to validate the function of these particular genes in the laboratory. Additionally, the stringent threshold used here may have excluded other AMGs.

Table 3. Putative auxiliary metabolic genes (AMGs) found in the *P. syringae* phage genomes classified into functional categories and comparative genomic analysis

Clones	CDS locus tag	Query length (aa)	Putative function category	Putative identified function	Phage hits*	Bacteria hits*	Organism best hit*	Best hit query coverage*	Best hit % identity*	Best hit E-value*	Number of Pseudomonas hits*
Aurca01	Pseudomonas_phage_Aurca01_00008	120	Cellular metabolism	glutamate 5-kinase	0	9	<i>Pseudomonas syringae</i> pv. <i>tomato</i>	1	100.00%	3E-84	9
Aurca01	Pseudomonas_phage_Aurca01_00028	181	Cellular metabolism	glycoside hydrolase family 19 protein	0	179	<i>Pseudomonas syringae</i> pv. <i>tomato</i>	1	97.24%	7E-62	178
Aurca01	Pseudomonas_phage_Aurca01_00088	123	Cellular metabolism	chemotaxis protein	2	425	<i>Pseudomonas viridiflava</i>	1	90.24%	9E-45	420
Cruim01	Pseudomonas_phage_Cruim01_00009	120	Cellular metabolism	glutamate 5-kinase	0	9	<i>Pseudomonas syringae</i> pv. <i>tomato</i>	1	100.00%	3E-84	9
Cruim01	Pseudomonas_phage_Cruim01_00028	181	Cellular metabolism	glycoside hydrolase family 19 protein	0	179	<i>Pseudomonas syringae</i> pv. <i>tomato</i>	1	97.24%	7E-62	178
Cruim01	Pseudomonas_phage_Cruim01_00082	123	Cellular metabolism	chemotaxis protein	2	425	<i>Pseudomonas viridiflava</i>	1	90.24%	9E-45	420
Nican01	Pseudomonas_phage_Nican01_00032	256	Cellular metabolism	PhoH-like protein	1	0	<i>Pseudomonas phage nickie</i>	1	94.14%	1E-89	0
Nican01	Pseudomonas_phage_Nican01_00067	146	Cellular metabolism	Photosystem I assembly protein Ycf4	1	0	<i>Pseudomonas phage phiK7B1</i>	1	76.71%	1E-54	0
Nican01	Pseudomonas_phage_Nican01_00150	143	Stress tolerance	tellurite resistance protein	1	0	<i>Pseudomonas phage phiK7B1</i>	1	98.60%	5E-20	0
Nican01	Pseudomonas_phage_Nican01_00074	280	Nucleic acid synthesis	dihydrofolate reductase	2	0	<i>Pseudomonas phage ZY21</i>	1	82.14%	9E-128	0
Nican01	Pseudomonas_phage_Nican01_00040	65	Cellular metabolism	von Willebrand factor type A domain protein	2	0	<i>Pseudomonas phage ZY21</i>	1	84.62%	2E-30	0
Nican01	Pseudomonas_phage_Nican01_00162	212	Cellular metabolism	ABC transporter	3	0	<i>Pseudomonas phage phiK7B1</i>	1	95.75%	6E-61	0
Nican01	Pseudomonas_phage_Nican01_00164	293	Cellular metabolism	putative ABC transporter ATP-binding protein aerobic	3	1	<i>Pseudomonas phage phiK7B1</i>	1	96.25%	0.0	1
Nican01	Pseudomonas_phage_Nican01_00048	407	Cellular metabolism	cobaltochelatase subunit aerobic	4	1	<i>Pseudomonas phage ZY21</i>	1	96.32%	1E-143	1
Nican01	Pseudomonas_phage_Nican01_00047	693	Cellular metabolism	cobaltochelatase subunit aerobic	4	0	<i>Pseudomonas phage phiK7B1</i>	1	87.91%	0.0	0
Pyxpy01	Pseudomonas_phage_Pyxpy01_00144	224	Stress tolerance	Integral membrane protein TerC family protein	1	0	<i>Pseudomonas phage REC</i>	0.99	77.03%	2E-58	0
Pyxpy01	Pseudomonas_phage_Pyxpy01_00084	76	Stress tolerance	Glutaredoxin	8	0	<i>Pseudomonas phage PE09</i>	1	90.79%	7E-22	0
Pyxpy01	Pseudomonas_phage_Pyxpy01_00146	215	Cellular metabolism	von Willebrand factor type A domain protein	9	0	<i>Pseudomonas phage PE09</i>	1	81.48%	3E-56	0
Pyxpy01	Pseudomonas_phage_Pyxpy01_00156	588	Nucleic acid synthesis	nicotinamide phosphoribosyltransferase	14	0	<i>Pseudomonas phage M5.1</i>	0.99	79.05%	0.0	0
Pyxpy02	Pseudomonas_phage_Pyxpy02_00144	224	Stress tolerance	Integral membrane protein TerC family protein	1	0	<i>Pseudomonas phage REC</i>	0.99	77.03%	2E-58	0
Pyxpy02	Pseudomonas_phage_Pyxpy02_00081	76	Stress tolerance	Glutaredoxin	8	0	<i>Pseudomonas phage PE09</i>	1	90.79%	7E-22	0
Pyxpy02	Pseudomonas_phage_Pyxpy02_00146	215	Cellular metabolism	von Willebrand factor type A domain protein	9	0	<i>Pseudomonas phage PE09</i>	1	81.48%	3E-56	0
Pyxpy02	Pseudomonas_phage_Pyxpy02_00156	588	Nucleic acid synthesis	nicotinamide phosphoribosyltransferase	14	0	<i>Pseudomonas phage M5.1</i>	0.99	79.05%	0.0	0
Touem01	Pseudomonas_phage_Touem01_00104	274	Cellular metabolism	ninC-like protein	1	0	<i>Caudoviricetes</i> sp.	0.92	77.87%	3E-94	0
Ulina01	Pseudomonas_phage_Ulina01_00029	151	Stress tolerance	aminoglycoside acetyltransferase	6	0	<i>Pseudomonas phage BUCT553</i>	1	98.01%	1E-28	0
Ulitu01	Pseudomonas_phage_Ulitu01_00028	151	Stress tolerance	aminoglycoside acetyltransferase	6	0	<i>Pseudomonas phage BUCT553</i>	1	98.68%	1E-26	0

*Threshold to report hits: 70% identity. 90% query coverage; □ The size of the phage genes with this symbol □ is believed to be complete based on homologous protein comparison with the bacteria gene size.

Also, even when proteins have low homology, their function can be conserved in phages. For instance, it has been demonstrated that the photosystem I sequence carried by phage PsaA differs from the photosystem I sequences carried by its cyanobacterial hosts (*Prochlorococcus* and *Synechococcus*), possibly due to recombination between the two hosts' sequences [73]. This threshold could be extended by including the presence of specific protein domains, whose function may be conserved despite divergence from the rest of the protein.

CONCLUSION

In spite of the renewed interest in phages as biocontrol agents against plant disease, the relative paucity of genetic and phenotypic data for phages of plant pathogenic bacteria makes it difficult to estimate their biogeographical distribution and potential as

biocontrol agents. The main objective of this study was to isolate a diverse range of phages from *P. syringae* and characterize their genome. It was hypothesized that increasing the number of enrichment strains would result in an extensive phage diversity. The results indicate that a wide genetic diversity of phages was successfully isolated. We have identified 25 new *P. syringae* phages, which belong to 18 new species in 14 genera, 11 of which are new. These genera are highly distinct from each other, with almost no inter-genomic homology (with the exception of two pairs of genera), indicating that the gene architectures and content are also highly specific to each genus. Three phage genera have been predicted to be temperate and possess genes that support this assumption. A discovery that requires further exploration and verification is the potentially new DNA packaging systems identified in the *Lyravirus sulafat* species. Finally, this study has highlighted diverse numerous potential AMGs, including genes involved in bacterial tellurite resistance, a toxic metalloid for organisms, which was previously found in the genome of phages from *P. syringae* pv. *actinidae*. The presence of these genes in the phage genome raises questions about their role in microbial metabolism and their implication in stress conditions in the host environment. This study increases the INPHARED databases of *P. syringae* phages by 23%, which remains relatively scarce compared to phages from *E. coli* and other more extensively studied bacterial species. Our genetic description of the phages provides a basis for future research into this host-virus system in agricultural ecosystems. Furthermore, a more comprehensive understanding of the genomics of *P. syringae* phages would allow a better assessment of their impact on the diversification and dynamics of the host population.

Funding information

This work was supported by the Plant Health and Environment Department of the French National Research Institute for Agriculture, Food and the Environment (INRAE) and Avignon University (AU).

Acknowledgements

We are grateful to I. Bornard head of the PACA centre's 3A microscopy platform for performing the TEM phage analysis. We also thank the UERI team in Gotheron for helping us to collect samples in the apricot orchards. We would like to express our gratitude to C. Persyn and H. Batina for their valuable advice on DNA extraction. Finally, we are thankful to G.H. Haustant, L. Ma. Biomics Platform, C2RT, Institut Pasteur, Paris, France, supported by France Génomique (ANR-10-INBS-09) and IBISA.

Conflicts of interest

The authors declare that there are no conflicts of interest.

References

- Suttle CA. Marine viruses – major players in the global ecosystem. *Nat Rev Microbiol* 2007;5:801–812.
- Middelboe M, Brussaard CPD. Marine viruses: key players in marine ecosystems. *Viruses* 2017;9:302.
- Williamson KE, Fuhrmann JJ, Wommack KE, Radosevich M. Viruses in soil ecosystems: an unknown quantity within an unexplored territory. *Annu Rev Virol* 2017;4:201–219.
- Mirzaei MK, Maurice CF. Ménage à trois in the human gut: interactions between host, bacteria and phages. *Nat Rev Microbiol* 2017;15:397–408.
- Blazanin M, Turner PE. Community context matters for bacteriophage ecology and evolution. *ISME J* 2021;15:3119–3128.
- Brown TL, Charity OJ, Adriaenssens EM. Ecological and functional roles of bacteriophages in contrasting environments: marine, terrestrial and human gut. *Curr Opin Microbiol* 2022;70:102229.
- Dong Z, Xing S, Liu J, Tang X, Ruan L, et al. Isolation and characterization of a novel phage Xoo-sp2 that infects *Xanthomonas oryzae* pv. *oryzae*. *J Gen Virol* 2018;99:1453–1462.
- Wang X, Wei Z, Yang K, Wang J, Jousset A, et al. Phage combination therapies for bacterial wilt disease in tomato. *Nat Biotechnol* 2019;37:1513–1520.
- Frampton RA, Taylor C, Holguín Moreno AV, Visnovsky SB, Petty NK, et al. Identification of bacteriophages for biocontrol of the kiwifruit canker phytopathogen *Pseudomonas syringae* pv. *actinidae*. *Appl Environ Microbiol* 2014;80:2216–2228.
- Vu NT, Kim H, Lee S, Hwang IS, Kwon C-T, et al. Bacteriophage cocktail for biocontrol of soft rot disease caused by *Pectobacterium* species in Chinese cabbage. *Appl Microbiol Biotechnol* 2023;108:11.
- Twort FW. An investigation on the nature of ultra-microscopic viruses. *The Lancet* 1915;186:1241–1243.
- D'Herelle F. On an invisible microbe antagonistic toward dysenteric bacilli: brief note by Mr. F. D'Herelle, presented by Mr. Roux. 1917. *Res Microbiol* 2007;158:553–554.
- Mallmann WL, Hemstreet C. Isolation of an inhibitory substance from plants; 1924. <https://naldc.nal.usda.gov/download/IND43966880/PDF> [accessed 22 August 2022].
- Coons GH, Kotila JE. The transmissible lytic principle (Bacteriophage) in relation to plant pathogens. *Phytopathology* 1925;15:357–370.
- Berge O, Monteil CL, Bartoli C, Chandeysson C, Guilbaud C, et al. A user's guide to A data base of the diversity of *Pseudomonas syringae* and its application to classifying strains in this phylogenetic complex. *PLoS One* 2014;9:e105547.
- Morris CE, Monteil CL, Berge O. The life history of *Pseudomonas syringae*: linking agriculture to earth system processes. *Annu Rev Phytopathol* 2013;51:85–104.
- Córdova P, Rivera-González JP, Rojas-Martínez V, Fiore N, Bastías R, et al. Phytopathogenic *Pseudomonas syringae* as a threat to agriculture: perspectives of a promising biological control using bacteriophages and microorganisms. *Horticulturae* 2023;9:712.
- Lamichhane JR, Varvaro L, Parisi L, Audergon J-M, Morris CE. Disease and frost damage of woody plants caused by *Pseudomonas syringae*. In: Sparks DL (ed). *Advances in Agronomy*. Academic Press; . pp. 235–295.
- Karimi-Kurdistani G, Harighi B. Phenotypic and molecular properties of *Pseudomonas syringae* pv. *syringae* the causal agent of bacterial canker of stone fruit trees in Kurdistan province. *J Plant Pathol* 2008;90:81–86.
- Donmez MF, Karlidag H, Esitken A. Identification of resistance to bacterial canker (*Pseudomonas syringae* pv. *syringae*) disease on apricot genotypes grown in Turkey. *Eur J Plant Pathol* 2010;126:241–247.
- Ivanova L. First occurrence of apricot blast disease caused by *Pseudomonas syringae* in the north-eastern part of Bulgaria. *Acta Hort* 2009;149–152.
- Giovanardi D, Ferrante P, Scortichini M, Stefani E. Characterisation of *Pseudomonas syringae* isolates from apricot orchards in north-eastern Italy. *Eur J Plant Pathol* 2018;151:901–917.

23. Parisi L, Morgaint B, Blanco-Garcia J, Guilbaud C, Chandeysson C, et al. Bacteria from four phylogroups of the *Pseudomonas syringae* complex can cause bacterial canker of apricot. *Plant Pathology* 2019;68:1249–1258.
24. Vasebi Y, Khakvar R, Tian L, Moubarak P, Valentini F, et al. Phenotypic characterization and phylogenetic analysis of *Pseudomonas syringae* strains associated with canker disease on apricot in Iran within the context of the global genetic diversity of the *P. syringae* complex. *Eur J Plant Pathol* 2020;158:545–560.
25. Skliros D, Papazoglou P, Gkizi D, Paraskevopoulou E, Katharios P, et al. In planta interactions of a novel bacteriophage against *Pseudomonas syringae* pv. tomato. *Appl Microbiol Biotechnol* 2023;107:3801–3815.
26. Warring SL, Malone LM, Jayaraman J, Easingwood RA, Rigano LA, et al. A lipopolysaccharide-dependent phage infects a pseudomonad phytopathogen and can evolve to evade phage resistance. *Environ Microbiol* 2022;24:4834–4852.
27. Crummett LT, Puxty RJ, Weihe C, Marston MF, Martiny JBH. The genomic content and context of auxiliary metabolic genes in marine cyanomyoviruses. *Virology* 2016;499:219–229.
28. Sun M, Yuan S, Xia R, Ye M, Balcázar JL. Underexplored viral auxiliary metabolic genes in soil: Diversity and eco-evolutionary significance. *Environ Microbiol* 2023;25:800–810.
29. Tamura K, Stecher G, Kumar S. MEGA11: Molecular evolutionary genetics analysis version 11. *Mol Biol Evol* 2021;38:3022–3027.
30. King EO, Ward MK, Raney DE. Two simple media for the demonstration of pyocyanin and fluorescein. *J Lab Clin Med* 1954;44:301–307.
31. Fortier L-C, Moineau S. Phage production and maintenance of stocks, including expected stock lifetimes. In: Clokie MRJ and Kropinski AM (eds). *Bacteriophages*. Totowa, NJ: Humana Press; . pp. 203–219.
32. Kropinski AM, Mazzocco A, Waddell TE, Lingohr E, Johnson RP. Enumeration of bacteriophages by double agar overlay plaque assay. *Methods Mol Biol* 2009;501:69–76.
33. Ackermann H-W. Basic phage electron microscopy. In: Clokie MRJ and Kropinski AM (eds). *Bacteriophages: Methods and Protocols, Volume 1: Isolation, Characterization, and Interactions*. Totowa, NJ: Humana Press; . pp. 113–126.
34. The Galaxy Community. The Galaxy platform for accessible, reproducible and collaborative biomedical analyses: 2022 update. *Nucleic Acids Res* 2022;50:W345–W351.
35. Bolger AM, Lohse M, Usadel B. Trimmomatic: a flexible trimmer for Illumina sequence data. *Bioinformatics* 2014;30:2114–2120.
36. Bankevich A, Nurk S, Antipov D, Gurevich AA, Dvorkin M, et al. SPAdes: a new genome assembly algorithm and its applications to single-cell sequencing. *J Comput Biol* 2012;19:455–477.
37. Garneau JR, Depardieu F, Fortier L-C, Bikard D, Monot M. PhageTerm: a tool for fast and accurate determination of phage termini and packaging mechanism using next-generation sequencing data. *Sci Rep* 2017;7:8292.
38. Lopes A, Tavares P, Petit M-A, Guérois R, Zinn-Justin S. Automated classification of tailed bacteriophages according to their neck organization. *BMC Genomics* 2014;15:1027.
39. Tynecki P, Guziński A, Kazimierczak J, Jadczyk M, Dastyh J, et al. PhageAI - bacteriophage life cycle recognition with machine learning and natural language processing. *bioRxiv* 2020. DOI: 10.1101/2020.07.11.198606.
40. Moraru C, Varsani A, Kropinski AM. VIRIDIC — a novel tool to calculate the intergenomic similarities of prokaryote-infecting viruses. *Viruses* 2020;12:1268.
41. Seemann T. Prokka: rapid prokaryotic genome annotation. *Bioinformatics* 2014;30:2068–2069.
42. Arndt D, Grant JR, Marcu A, Sajed T, Pon A, et al. PHASTER: a better, faster version of the PHAST phage search tool. *Nucleic Acids Res* 2016;44:W16–21.
43. Cook R, Brown N, Redgwell T, Rihtman B, Barnes M, et al. Infrastructure for a PHAge reference database: identification of large-scale biases in the current collection of cultured phage genomes. *PHAGE* 2021;2:214–223.
44. Ceysens P-J, Lavigne R. Bacteriophages of *Pseudomonas*. *Future Microbiol* 2010;5:1041–1055.
45. De Smet J, Hendrix H, Blasdel BG, Danis-Wlodarczyk K, Lavigne R. *Pseudomonas predators*: understanding and exploiting phage-host interactions. *Nat Rev Microbiol* 2017;15:517–530.
46. Rabiey M, Roy SR, Holtappels D, Franceschetti L, Quilty BJ, et al. Phage biocontrol to combat *Pseudomonas syringae* pathogens causing disease in cherry. *Microb Biotechnol* 2020;13:1428–1445.
47. Morris CE, Sands DC, Vanneste JL, Montarry J, Oakley B, et al. Inferring the evolutionary history of the plant pathogen *Pseudomonas syringae* from its biogeography in headwaters of rivers in North America, Europe, and New Zealand. *mBio* 2010;1:e00107-10.
48. Monteil CL, Lafolie F, Laurent J, Clement J-C, Simler R, et al. Soil water flow is a source of the plant pathogen *Pseudomonas syringae* in subalpine headwaters. *Environ Microbiol* 2014;16:2038–2052.
49. Turner D, Kropinski AM, Adriaenssens EM. A roadmap for genome-based phage taxonomy. *Viruses* 2021;13:506.
50. Silva EC, Rodrigues LMR, Vila MMDC, Balcão VM. Newly isolated phages preying on *Pseudomonas syringae* pv. *garcae*: In vitro and ex vivo inactivation studies in coffee plant leaves. *Enzyme Microb Technol* 2023;171:110325.
51. Rocha EPC, Danchin A. Base composition bias might result from competition for metabolic resources. *Trends Genet* 2002;18:291–294.
52. Backman T, Latorre SM, Symeonidi E, Muszyński A, Bleak E, et al. A weaponized phage suppresses competitors in historical and modern metapopulations of pathogenic bacteria. *bioRxiv* 2024. DOI: 10.1101/2023.04.17.536465.
53. López-Leal G, Camelo-Valera LC, Hurtado-Ramírez JM, Verleyen J, Castillo-Ramírez S, et al. Mining of thousands of prokaryotic genomes reveals high abundance of prophages with a strictly narrow host range. *mSystems* 2022;7:e0032622.
54. Baltrus DA, Weaver S, Krings L, Nguyen AE. Genomic correlates of tailocin sensitivity in *Pseudomonas syringae*. *Microbiology* 2023. DOI: 10.1101/2023.04.24.538177.
55. Shen A, Millard A. Phage genome annotation: where to begin and end. *PHAGE* 2021;2:183–193.
56. Young R. Phage lysis: three steps, three choices, one outcome. *J Microbiol* 2014;52:243–258.
57. Berry J, Summer EJ, Struck DK, Young R. The final step in the phage infection cycle: the Rz and Rz1 lysis proteins link the inner and outer membranes. *Mol Microbiol* 2008;70:341–351.
58. Bailly-Bechet M, Vergassola M, Rocha E. Causes for the intriguing presence of tRNAs in phages. *Genome Res* 2007;17:1486–1495.
59. Taslem Mourosi J, Awe A, Guo W, Batra H, Ganesh H, et al. Understanding bacteriophage tail fiber interaction with host surface receptor: the key “blueprint” for reprogramming phage host range. *Int J Mol Sci* 2022;23:12146.
60. Meyer JR, Dobias DT, Medina SJ, Servilio L, Gupta A, et al. Ecological speciation of bacteriophage lambda in allopatry and sympatry. *Science* 2016;354:1301–1304.
61. de Leeuw M, Baron M, Ben David O, Kushmaro A. Molecular insights into bacteriophage evolution toward its host. *Viruses* 2020;12:1132.
62. Ohlendorf DH, Tronrud DE, Matthews BW. Refined structure of Cro repressor protein from bacteriophage λ suggests both flexibility and plasticity. *J Mol Biol* 1998;280:129–136.
63. Ramesh N, Archana L, Madurantakam Royam M, Manohar P, Eniyan K. Effect of various bacteriological media on the plaque morphology of *Staphylococcus* and *Vibrio* phages. *Access Microbiology* 2019;1:e000036.
64. Millard A, Clokie MRJ, Shub DA, Mann NH. Genetic organization of the psbAD region in phages infecting marine *Synechococcus* strains. *Proc Natl Acad Sci USA* 2004;101:11007–11012.

65. Zheng X, Jahn MT, Sun M, Friman V-P, Balcazar JL, *et al.* Organochlorine contamination enriches virus-encoded metabolism and pesticide degradation associated auxiliary genes in soil microbiomes. *ISME J* 2022;16:1397–1408.
66. Pérez-Arellano I, Rubio V, Cervera J. Dissection of *Escherichia coli* glutamate 5-kinase: functional impact of the deletion of the PUA domain. *FEBS Lett* 2005;579:6903–6908.
67. Ping D, Wang T, Fraebel DT, Maslov S, Sneppen K, *et al.* Hitchhiking, collapse, and contingency in phage infections of migrating bacterial populations. *ISME J* 2020;14:2007–2018.
68. Sharon I, Alperovitch A, Rohwer F, Haynes M, Glaser F, *et al.* Photosystem I gene cassettes are present in marine virus genomes. *Nature* 2009;461:258–262.
69. Mann NH, Cook A, Millard A, Bailey S, Clokie M. Bacterial Photosynthesis genes in a virus. *Nature* 2003;424:741.
70. Clokie MRJ, Shan J, Bailey S, Jia Y, Krisch HM, *et al.* Transcription of a “photosynthetic” T4-type phage during infection of a marine cyanobacterium. *Environ Microbiol* 2006;8:827–835.
71. Taylor DE. Bacterial tellurite resistance. *Trends Microbiol* 1999;7:111–115.
72. Peng W, Wang Y, Fu Y, Deng Z, Lin S, *et al.* Characterization of the tellurite-resistance properties and identification of the core function genes for tellurite resistance in *Pseudomonas citronellolis* SJTE-3. *Microorganisms* 2022;10:95.
73. Mazor Y, Greenberg I, Toporik H, Beja O, Nelson N. The evolution of photosystem I in light of phage-encoded reaction centres. *Philos Trans R Soc Lond B Biol Sci* 2012;367:3400–3405.

The Microbiology Society is a membership charity and not-for-profit publisher.

Your submissions to our titles support the community – ensuring that we continue to provide events, grants and professional development for microbiologists at all career stages.

Find out more and submit your article at microbiologyresearch.org